IVYSPRING INTERNATIONAL PUBLISHER

International Journal of Medical Sciences

2018; 15(13): 1423-1432. doi: 10.7150/ijms.27867

Research Paper

Administration of $CoCl_2$ Improves Functional Recovery in a Rat Model of Sciatic Nerve Transection Injury

Shuai An✉, Meng Zhou, Zheng Li, Mingli Feng, Guanglei Cao, Shibao Lu, Limin Liu

Department of Orthopedics, Xuanwu Hospital, Capital Medical University

✉ Corresponding author: Shuai An, MD, PhD, Department of Orthopedics, Xuanwu Hospital, Capital Medical University, 45 Changchun Street, Beijing 100053, P.R. China. Email: anshuai@xwh.ccmu.edu.cn

Received: 2018.06.13; Accepted: 2018.08.29; Published: 2018.09.07

Abstract

Peripheral nerve injury is known to activate the hypoxia-inducible factor-1α (HIF-1α) pathway as one of pro-regenerative transcriptional programs, which could stimulate multiple injury-induced gene expression and contribute to axon regeneration and functional recovery. However, the role of HIF-1α in peripheral nerve regeneration remains to be fully elucidated. In this study, rats were divided into three groups and treated with sham surgery, surgery with cobalt chloride ($CoCl_2$) and surgery with saline, respectively. Sciatic functional index, morphologic evaluations of muscle fibers, and never conduction velocity were performed to measure the functional recovery at 12 weeks postoperatively. In addition, the effects of $CoCl_2$ on the expression of HIF-1α, glial cell line-derived neurotrophic factor (GDNF), brain-derived neurotrophic factor (BDNF) and nerve growth factor (NGF) were determined at mRNA levels; as well as HIF-1α, the dual leucine zipper kinase (DLK), the c-Jun N-terminal kinase (JNK), phosphorylated JNK (p-JNK), BDNF and NGF were measured at protein level at 4 weeks postoperatively. Systemic administration of $CoCl_2$ (15 mg/kg/day intraperitoneally) significantly promoted functional recovery of rats with sciatic nerve transection injury. This study demonstrated in rats treated with $CoCl_2$, the expression of HIF-1α, GDNF, BDNF and NGF was significantly increased at mRNA level, while HIF-1α, DLK, p-JNK, BDNF and NGF was significantly increased at protein level.

Key words: peripheral nerve injury, nerve regeneration, hypoxia, hypoxia-inducible factor-1α, $CoCl_2$

Introduction

Peripheral nerve injury (PNI) is one of the most common reasons for permanent disabilities in clinical practice [1]. Although peripheral nerve system neuron could active pro-regenerative transcriptional program and enable axon regeneration compared with central nerve system, complete recovery is only occasionally achieved after a nerve injury and, in many cases, the clinical functional recovery is rather unsatisfactory after transection injury due to many activated complicated pathophysiologic process and the unclear activation mechanisms of pro-regenerative state after PNI [2, 3]. In order to answer the question how to activate a pro-regenerative program, many transcriptional profile studies focused on screening the potential regeneration-associated genes (RAGs) [4-7]. Hypoxia-Inducible Factor (HIF) was identified through comparison between four lists of transcription factors in regenerating dorsal root ganglia.

HIF pathway is the central pathway for sensing and responding to alterations in oxygen levels in nearly all extant metazoan species analyzed [8, 9]. HIF-1 consisted of HIF-1α and HIF-1β subunits, which plays an essential role in the cellular response to hypoxia [10]. Considering that HIF-1β is present in excess, HIF-1α protein levels determine HIF-1 transcriptional activity [9]. Recently, it has been reported that HIF-1α plays a critical transcriptional regulator in peripheral nerve regeneration, which suggests hypoxia as a tool to promote axon regeneration [11] and injured nerve functional recovery [12, 13]. Meanwhile, it has been also reported

that HIF-1α may be related with tumor development and neuralgic formation [14]. A more thorough understanding of hypoxia in nerve regeneration will lead to the elucidation of activation mechanisms of pro-regeneration program that may helpful in the development of protective therapies.

Cobalt chloride ($CoCl_2$), known as a mimicking agent of hypoxia, was shown to alter several systemic mechanisms related to hypoxia [15-19] and up-regulate HIF-1α [20, 21]. Chemically, $CoCl_2$ reacts with oxygen decreasing its dissolution and oxygenation of aqueous solutions, being a way of inducing unavailability of oxygen [22]. Besides, cobalt could not only increase the stabilization of HIF-1α and downstream target genes by inhibiting prolyl hydroxylase enzymes, thus preventing its degradation [23], but also, as a chelator, could replace of Fe^{2+} in hemoglobin, which impairs cell's reception of oxygen [21]. In previous studies, $CoCl_2$ was used to establish different hypoxia models both in vivo [24] and in cell culture [16, 21]. An improved understanding of the changes in functional recovery process and gene expression induced by $CoCl_2$ during sciatic nerve transection injury regeneration in animals might help advancement in transforming $CoCl_2$ as an efficacious therapeutic regimen in human and helping improve rehabilitation after PNI.

In the present study, it was hypothesized that sciatic nerve transection injury (SNT) treated with $CoCl_2$ may exhibit better functional recovery. To determine whether systemic application of $CoCl_2$ improve the injured peripheral nerve regeneration in a rat model, the effects of $CoCl_2$ were evaluated on sciatic functional index (SFI), muscular mass and morphology, neuroelectrophysiological parameters at 12 weeks after nerve injury.

Materials and Methods

Animal care

Experiments were performed using 45 specific pathogen-free female Sprague-Dawley rats with a body weight of 200-250 g at the age of eight-weeks, which were obtained from the Laboratory Animal Center of Capital Medical University (Beijing, China). The rats were maintained under humidity (50-60%) and temperature (23-25 °C) controlled conditions with a 12-hours light/dark cycle at the Central Animal Facility, Capital Medical University (Beijing, China). Experimental procedures were reviewed and approved by the Ethics Committee of Xuan Wu Hospital, Capital Medical University.

Animal experiments

All animals were allowed 1-week acclimatization to local conditions and had free access to untreated tap water and standard rat chow. Then the rats were randomly divided into three experimental groups for the subsequent interventions: i) Sham group was treated with a surgical procedure only to expose sciatic nerve; ii) Model group was treated with intraperitoneal injection of $CoCl_2$ (15 mg/kg/day) for 14 days, as described previously[8], and began 2 hours after sciatic nerve transection injury and iii) Control group was treated with intraperitoneal injection of saline (15 mg/kg/day) for 14 days and began 2 hours after sciatic nerve transection injury (Fig. 1B).

All surgical procedures of sciatic nerve axotomy were performed under a microscope. The rats were anaesthetized through intraperitoneal injection of sodium pentobarbital (30 mg/kg). Following complete anesthesia, skin preparation and

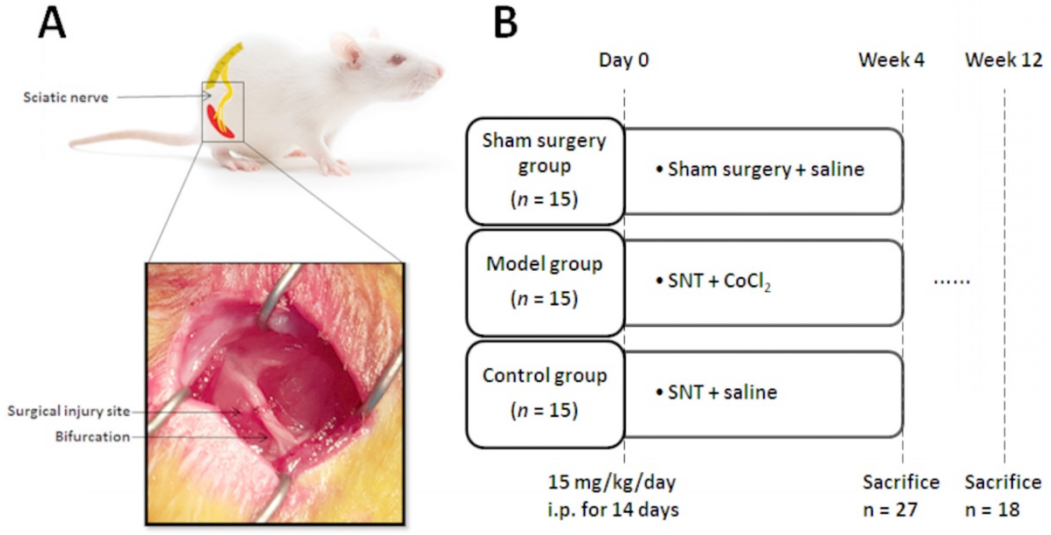

Figure 1. (A) Schematic diagram and photo of the surgical procedure. The sciatic nerve was severed at 5 mm upon the bifurcation site. (B) Experimental protocols. SNT: sciatic nerve transection injury, and i.p.: intraperitoneal injection.

disinfection were carried out in the right hind limb. The right sciatic nerve and its two main branches (common peroneal nerve and tibial nerve) were fully exposed. The sciatic nerve was severed at 5 mm upon the bifurcation site. Then the severed sciatic nerve was repaired through anastomosis of two stumps with 10-0 nylon suture, and the incision was subsequently closed with 4-0 suture (Fig. 1A).

The rats were sacrificed by cervical dislocation under anesthesia at 4 weeks after surgery and sciatic nerves were harvested for reverse transcription-quantitative polymerase chain reaction (RT-qPCR), western blot, the enzyme-linked immunosorbent assay (ELISA) to evaluate the changes of HIF-1α and its downstream target genes [8, 11]. SFI, neuroelectrophysiological examinations and H&E staining were performed at 12 weeks after surgery, according to previous studies [2, 25, 26].

SFI analysis

To assess lower limb function, the SFI was measured as previously described [26, 27]. At 12 weeks after SNT, rats were allowed conditioning trials in a confined walking track (10 × 60 cm) darkened at one end. White papers were placed on the bottom of the track. The hindpaws were dippep in black ink and footprints were appeared immediately on the papers when the rats walked down the track. The following parameters were recorded: print length (distance from heel to toe, PL), toe spread (distance from first to fifth toe, TS), and intermediary toe spread (distance from second to fourth toe, IT). PL, TS, and IT were collected on both the left normal (N) and the right experimental (E) hind legs.

$$SFI = -38.3 \times (EPL - NPL) + 109.5 \times (ETS - NTS) / NTS + 13.3 \times (EIT - NIT) / NIT - 8.8$$

The SFI was calculated according to Bain-Mackinnon-Hunter formula and scores varied from 0 to -100 (Fig. 2A).

Neuroelectrophysiological examination

The Nerve conduction velocity (NCV) of sciatic nerve was measured through Medlec Synergy Electrophysiological System (Oxford Instrument Inc., Oxford, UK). The repaired sciatic nerve was exposed at 12 weeks after the surgery. For electrical stimulation and recording, two monopolar 12 mm length and 0.35 mm diameter teflon needle electrodes were used. The tips of the stimulus electrodes were curved beforehand for better fit and to prevent injuries. A monopolar electrode was used as a reference (neutral) electrode, but it was positioned at the midpoint between the stimulation and the recording electrodes. Single electrical pulses were delivered via stimulation electrode placed in turn at the proximal and distal trunk of the regenerated nerve and electromyography was recorded by inserting the recording electrode into the belly of gastrocnemius muscle. Paraffin oil was applied around the nerve trunk to reduce bypass conduction through the liquid. The stimulation signal was a square wave, with an intensity of 0.9 mA, a wave width of 0.1 ms and a frequency of 1 Hz. If impedance exceeded five Ω, the electrodes were relocated or replaced. The latency of electromyography was obtained. Also, the difference in latency of electromyography was measured, and the distance between the proximal and distal sites of simulation was recorded to calculate the conduction velocity across the regenerated nerve (Fig. 3A). The stimulation intensity was gradually strengthened until the amplitude of the compound muscle action potential (CMAP) wave ceased to progressively increase and a generally identical shape for the CMAP wave was formed from the stimulation at both the distal and proximal stumps. The amplitude of the

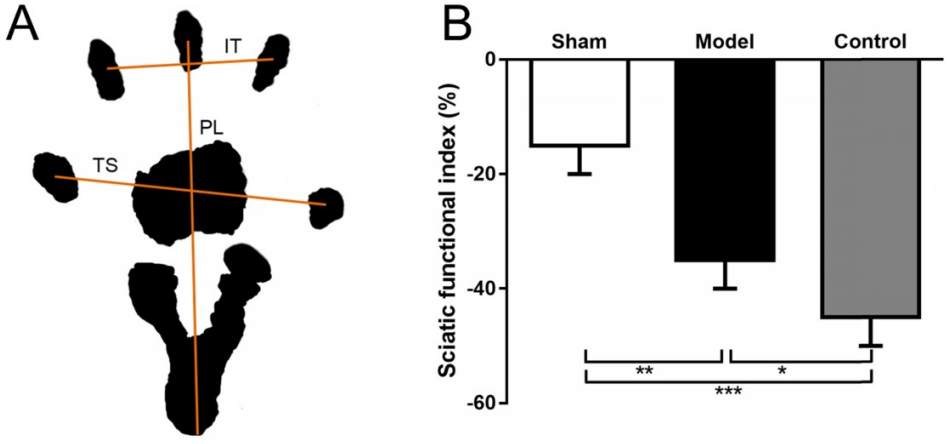

Figure 2. (A) Representation of the parameter in calculating the SFI after obtaining the animals' footprints. Print length (PL), distance from heel to toe. Toe spread (TS), distance from first to fifth toe. And intermediary toe spread (IT), distance from second to fourth toe. (B) SFI in sham group (sham surgery + saline) and model group (SNT + $CoCl_2$) was better than that in control group (SNT + saline). SFI: sciatic functional index. * $p < 0.05$. ** $p < 0.01$.

proximal CMAP was recorded, which was the distance from the initiation point to the negative peak (upward) of the wave (Fig. 3A) [28].

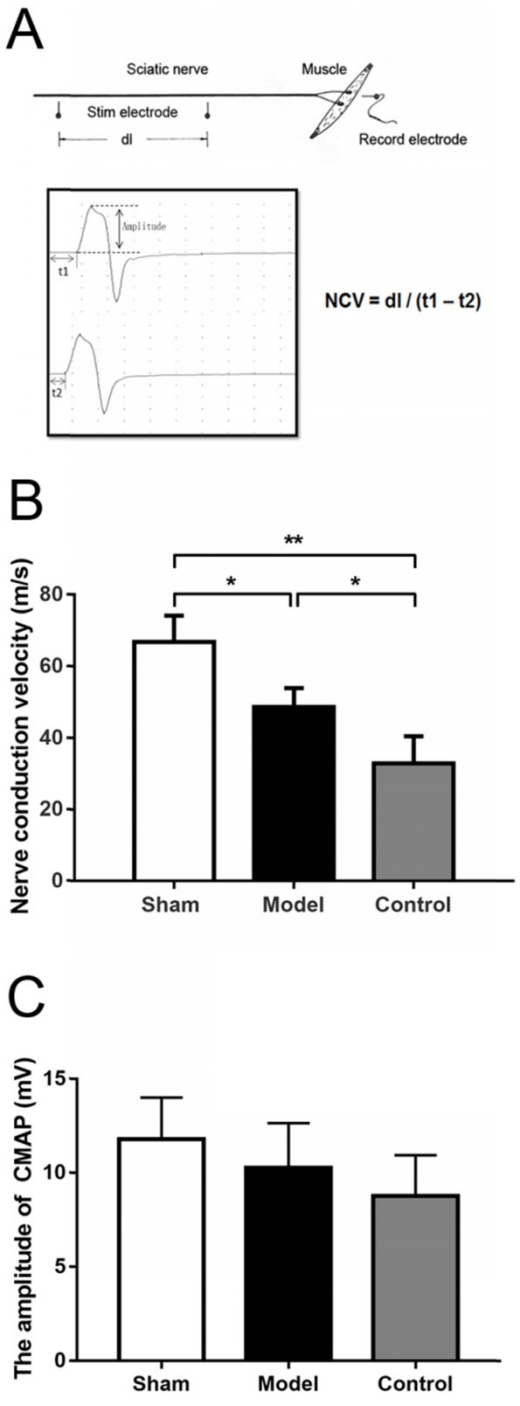

Figure 3. (A) Schematic diagram of NCV by electrophysiological examination. The stimulating electrodes were placed in two proximal point and the distance between two points was recorded (dl). The recording electrode was place in the gastrocnemius muscle. After stimulating two points respectively, the conduction latent time and electromyography were recorded (t1 & t2). NCV was calculated as the equation. The amplitude was the distance from the initiation point to the negative peak (upward) of the wave. (B) NCV in sham group (sham surgery + saline) and model group (SNT + $CoCl_2$) were higher than that in control group (SNT + saline) with significant difference. (C) The compound muscle action potential indicated that the wave amplitudes in sham group, model group and control group were not statistically significant difference ($p = 0.1002$). NCV: nerve conduction velocity. * $p < 0.05$. ** $p < 0.01$.

Wet muscle weight and histomorphometric evaluation

The gastrocnemius was known as an important muscle innervated by the sciatic nerve [2, 26, 29]. The whole gastrocnemius was isolated by severing it at its starting and ending points. The wet muscle weight of bilateral gastrocnemius and wet weight ratios of the experimental side to the normal side was measured using an electronic balance immediately after sacrificing of animals at 12 weeks postoperatively [29]. Transverse sectioning of the muscle samples was performed with hematoxylin and eosin (H&E) staining after fixing with paraformaldehyde, dehydrating with graded ethanol and embedding in paraffin wax. Ten out of 100 cross-sections per muscle were photographed at 10 × 5 magnification (necessary to comprise the entire diameter of the muscle). Five fields per cross-section were obtained under a magnification of 10 × 40 in the upper left, lower left, upper right, lower right and central field of the selected cross-sections of the muscle fiber for quantification using Image Pro Plus 6.0 (Media Cybernetics Inc., Rockville, MD, USA). The diameter of muscular fiber and cross-sectional area of H&E stained sections (5 μm) of the gastrocnemius were examined and approximately 250 muscle fibers per rat were evaluated [30]. The diameter of muscular fiber was measured as the minimal 'Feret's diameter' which is the minimum distance of parallel tangents at opposing borders of the muscle fiber [31].

RNA extraction and RT-qPCR

Total RNA was extracted from fresh nerve tissues of each group using the TRIzol reagent according to the manufacturer's instructions (Invitrogen Life Technologies, Carlsbad, CA, USA). RNA quantity and quality were determined by using the NanoDrop 2000 Spectrophotometer (Thermo Fischer Scientific, Waltham, MA, USA). Total RNA was reverse-transcribed using the PureLink RNA mini Kit following the manufacturer's instructions (Thermo Fischer Scientific, Waltham, MA, USA). RT-qPCR was performed to measure mRNA expression levels relative to Glyceraldehyde-3-Phosphate Dehydrogenase (GAPDH) mRNA expression with the ABI ViiA 7 Real Time PCR System (Thermo Fischer Scientific, Waltham, MA, USA) using Fast SYBR Green Master Mix (Thermo Fischer Scientific, Waltham, MA, USA). The primers used were as following: HIF-1α, 5'-GTCCCAGCTACGAA GTTACAGC-3' (forward) and 5'-CAGTGCAGGAT ACACAAGGTTT-3' (reverse); vascular endothelial growth factor (VEGF), 5'-CTGCCGTCCGATTGAG ACC-3' (forward) and 5'-CCCCTCCTTGTACCACTG TC-3' (reverse); glial cell line-derived neurotrophic

factor (GDNF), 5′-TCCAACTGGGGGTCTACGG-3′ (forward) and 5′-GCCACGACATCCCATAACTTC AT-3′ (reverse); brain-derived neurotrophic factor (BDNF), 5′-TCATACTTCGGTTGCATGAAGG-3′ (forward) and 5′-AGACCTCTCGAACCTGCCC-3′ (reverse); nerve growth factor (NGF), 5′-CCAGT GAAATTAGGCTCCCTG-3′ (forward) and 5′-CCTT GGCAAAACCTTTATTGGG-3′ (reverse); and GAPDH, 5′-TGACCTCAACTACATGGTCTACA-3′ (forward) and 5′-CTTCCCATTCTCGGCCTTG-3′ (reverse). Primers were synthesized by 100 Biotech (Hangzhou, China). The PCR thermal cycling conditions were as follows: 95°C for 15 secs and 60°C for 1 min. All experiments were performed in triplicate and repeated a minimum of three times. The RT-qPCR results were expressed relative to gene expression levels at the threshold cycle (Ct) and were related to the control.

Western blot analysis

Radioimmunoprecipitation assay buffer containing protease inhibitors (Sigma-Aldrich, St. Louis, MO, USA) was used to prepare tissue lysates with 1% SDS. Protein quantification was performed using a BCA Protein Assay Kit (Beyotime, Shanghai, China). Total proteins were resolved on 10% SDS-PAGE and electrotransferred onto Hydrophobic PVDF Transfer Membrane (MilliporeSigma, Temecula, CA, USA). The membranes were blocked in 5% skimmed milk in Tris-buffered saline containing 0.1% Tween 20 (TBST) for 30 min and incubated overnight at 4°C with primary rabbit polyclonal antibodies against HIF-1α (cat. no. AF1009; Affinity), VEGF (cat. no. AF5131; Affinity), DLK-1 (cat. no. AP20860c; Abgent), p-JNK (cat. no. AF3318; Affinity), JNK (cat. no. AF6318; Affinity), and GAPDH (cat. no. A01020; Abbkine). All antibodies were diluted 1:1,000 in Tris-buffered saline. Blots were washed in TBST and labeled with horseradish peroxidase-conjugated secondary antibody (Cell Signaling Technology, Inc., Danvers, MA, USA). Bands and band intensity were detected and calculated using chemiluminescence (Thermo Fisher Scientific, Waltham, MA, USA) and Image Quant LAS4000 (GE Healthcare Life Sciences, Little Chalfont). The Protein expression levels were expressed related to GAPDH levels [32, 33].

ELISA

The protein levels of BDNF and NGF were evaluated using BDNF ELISA Kit (cat. no. RA20017; Bio-Swamp) and NGF ELISA Kit (cat. no. RA20135; Bio-Swamp) following the manufacturer's instructions. The absorbance was measured using a plate reader (BioTek Elx800) at 450 nm with an absorbance correction at 540 nm. The concentration was calculated based on the standard curve and expressed in absolute terms (pg/ml).

Statistical analysis

Statistical analyses were performed using SPSS 19.0 (SPSS Inc., Chicago, IL, USA). Values are expressed as the mean ± standard deviation. An independent *t*-test was adopted for two-group comparison, and one-way analysis of variance (One-way ANOVA) was used for multi-group comparison. Comparison between the groups was made by analyzing data with a post-hoc method Tukey. Enumeration data were analyzed using a chi-square test. Statistical significance was established as $p < 0.05$.

Results

$CoCl_2$ accelerates functional recovery of injured sciatic nerve during nerve regeneration.

SFI of walking track test, parameters of neuroelectrophysiological examinations, and wet weight and morphology of muscular fiber were performed to evaluate the effects of functional recovery for hypoxia induced by $CoCl_2$ during peripheral nerve regeneration at week 12 postoperatively.

Walking track analysis of rats that did not have ulcers and toe self-biting showed that the SFI in the sham group was significantly higher compared with the model group ($p = 0.0065$) and the control group ($p = 0.0008$). Although the value in the model group was also higher than that in the control group, there is no significant difference between two groups ($p = 0.1089$) (Fig. 2B).

Electrophysiological examination was performed with fully anaesthetized rats. The NCVs in the sham group were significantly greater than that in the model and the control group (66.7 ± 7.41 vs 48.6 ± 5.33, $p = 0.0402$; 66.7 ± 7.41 vs 32.9 ± 7.52, $p = 0.0022$), While the value of the model group was also higher than that of the control group but without significant difference ($p = 0.0684$) (Fig. 3B). The compound muscle action potential indicated that the wave amplitudes were 11.80 ± 2.22 mV, 10.28 ± 2.38 mV and 8.77 ± 2.18 mV in sham group, model group and control group, respectively, but this was not statistically significant difference ($p = 0.1002$).

There were no significant differences among the wet weights of normal side in three groups at 12 weeks after surgery (2.12 ± 0.21 vs 1.98 ± 0.10 vs 1.80 ± 0.20, $p = 0.1658$). The wet weights of experimental side in control group were slightly less than those of the

other two groups (1.86 ± 0.08 vs 1.29 ± 0.15 vs 0.91 ± 0.25, p = 0.0016). The wet weight ratio of the experimental side to the normal side were 88.7 ± 12.13%, 64.75 ± 4.72% and 53.9 ± 14.02% in sham group, model group and control group, respectively; The wet weight ratio of control group were less than those of the other two groups (p = 0.0214) (Fig. 4D). H& E staining showed that cross-sectional diameter of sham group was approximately 34.5 ± 3.1 μm, with distinct borders and uniform staining (Fig. 4A). The muscle fibers of control group displayed atrophy caused by prolonged denervation, with uneven staining (Fig. 4C). The diameter of muscle fiber in sham group is thicker than the control group with significant difference (p = 0.0131), while diameters in model group had no significant differences with sham and control groups (29.4 ± 1.8 vs 34.5 ± 3.1, p =0.0765; 29.4 ± 1.8 vs 26.6 ± 1.7, p = 0.3566) (Fig. 4E). Besides, the average cross-section area was 895.2 ± 94.6, 668.5 ± 76.3 and 487.7 ± 65.7 μm^2 in the sham group, model group and control group, respectively (Fig. 4F). There were significant differences of cross-section area among three groups (p < 0.0001).

The HIF-1 pathway is functional and mediates hypoxia-induced gene expression during nerve regeneration under hypoxia.

Hypoxia is one of the most important pathological changes during nerve injuries. As we know, it is common that nerve injury can increase the metabolic level of the nerve, leading to increased oxygen consumption and local hypoxia during nerve repair. Induction of HIF-1α using $CoCl_2$ to mimic the effects of hypoxia is a reliable method [8, 15]. In the present study, the mRNA levels of HIF-1α were analyzed using RT-qPCR and presented in Fig. 5. Rats treated with $CoCl_2$ exhibited a significantly increased HIF-1α expression. In addition, it was observed that the protein levels of HIF-1α were increased at week 4 (Fig. 6). To further access whether HIF-1α had a direct functional role in this process, the expression of downstream genes was investigated using RT-qPCR, western blot analysis and ELISA test. The results also indicated that $CoCl_2$ significantly increased NGF, BDNF and GDNF on both mRNA level and protein level, as well as DLK, JNK and p-JNK on protein level (Figs. 5 and 6). These results suggested that the effect of $CoCl_2$ on nerve repair may involve in the activation of HIF-1α signaling pathway.

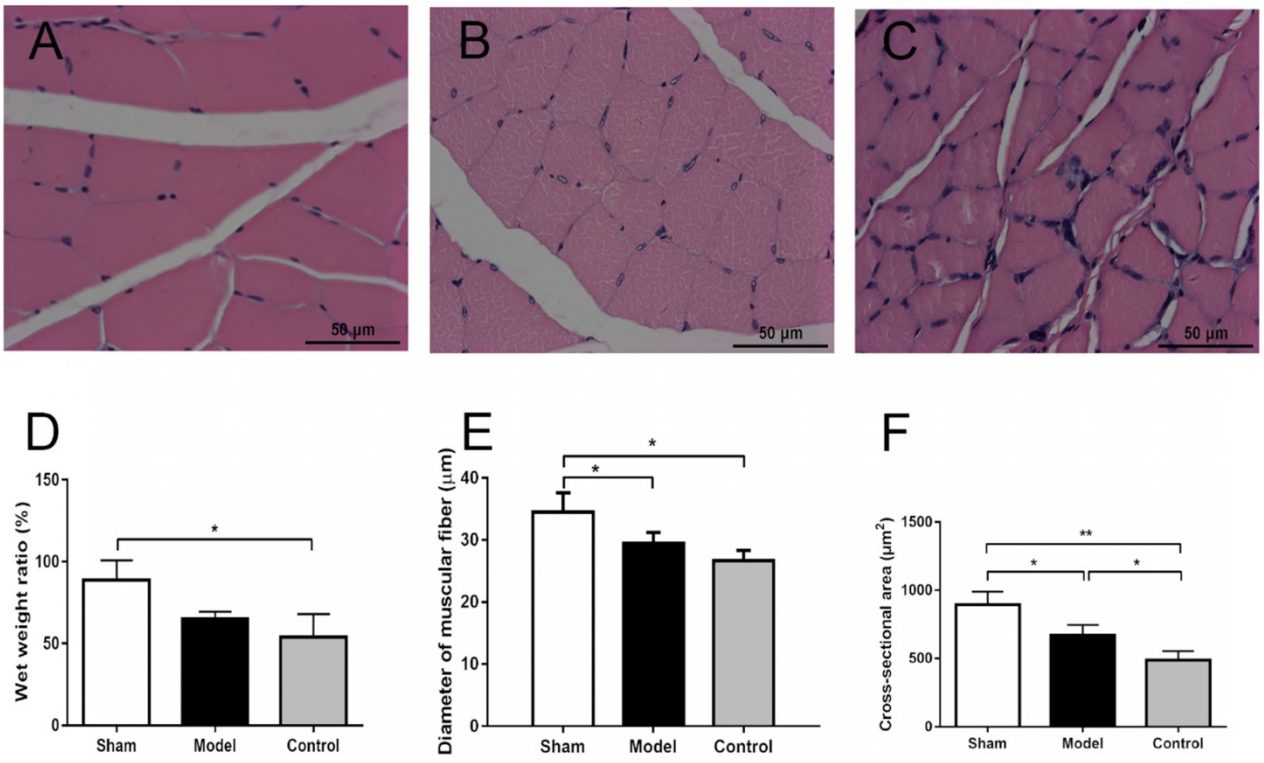

Figure 4. The cross-section morphology of the muscle fibers (10 × 40) and the comparison of fiber diameters in three groups. (A) Sham group (sham surgery + saline): Muscle fibers are evenly arranged, regular in shape, and thicker in diameter. (B) Model group (SNT + $CoCl_2$): Muscle fiber shape is basically regular, smaller diameter. (C) Control group (SNT + saline): Muscle fibers are relatively regular and have the smallest diameter. (D) The wet weight ratio of the experimental side to the normal side were 88.7 ± 12.13%, 64.75 ± 4.72% and 53.9 ± 14.02% in sham group, model group and control group, respectively; The wet weight ratio of control group were less than those of the other two groups (p = 0.0214). (E) The diameter of muscle fiber in sham group is thicker than the other two groups with significant difference, while diameter in model group was thicker than that in control group but without significant difference. (F) Cross-section areas were 895.2 ± 94.6, 668.5 ± 76.3 and 487.7 ± 65.7 μm2 in the sham group, model group and control group, respectively. There were significant differences of cross-section area among three groups (p < 0.0001). SNT: sciatic nerve transection injury. * p < 0.05. ** p < 0.01. *** p < 0.001.

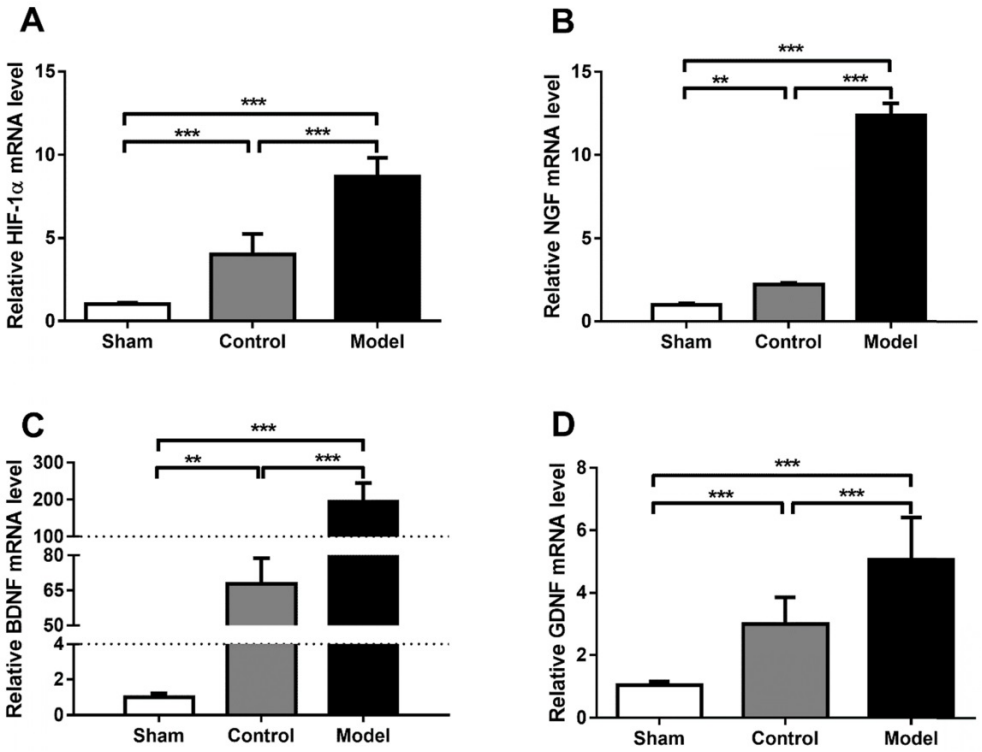

Figure 5. Quantification of HIF-1α, NGF, BDNF and GDNF mRNA level (A-D). $CoCl_2$ significantly increased HIF-1α, NGF, BDNF and GDNF on mRNA level in model group (SNT + $CoCl_2$), which has statistical difference with sham group (sham surgery + saline) and control group (SNT + saline). The data were analyzed by one-way ANOVA followed by a post-hoc method Student-Newman-Keuls (S-N-K). Graphs show indicate mean ± SD. HIF-1α: hypoxia inducible factor 1α; NGF: nerve growth factor; BDNF: brain-derived neurotrophic factor; GDNF: glial cell line-derived neurotrophic factor. ** $p < 0.01$. *** $p < 0.001$.

Discussion

Peripheral nerve regeneration is a complex process involving restoring the interrupted neuronal connectivity and resulting in functional recovery [34]. Treatments for nerve transection injury have addressed a variety of scientific disciplines, including reconstructive microsurgery, transplantation, biomaterial science, physical therapy, and genetic pharmacotherapy [35-37]. Previous studies have demonstrated that hypoxic stress may induce the expression of multiple genes and affect functional recovery of axon regeneration through HIF pathway [11, 13, 14, 38, 39]. Our study indicates that mimicking hypoxia status with $CoCl_2$ improves functional recovery of axon regeneration in sciatic nerve injury model and that HIF-1α contributes to regulate a large ensemble of transcriptional responses following axotomy. Here we demonstrated that the expression of neurotrophic factors including NGF, BDNF and GDNF could be upregulated by HIF-1α, while DLK, JNK and p-JNK could be induced during nerve regeneration. This provides a potential non-invasive but effective strategy for activating the pro-regenerative program and improving regeneration of injured nerve.

In this study, the functional recovery of sciatic nerve transection injury models was measured by morphologic examination of reinnervated muscles and neuroelectrophysiological examination of injured nerves. We found that SFI, NCV, the wave amplitude in model group were better than those in control group, but there was no significant difference. At the same time, these parameters in both model group and control group were significant less than those in sham group. As we know, NCV is a local indicator of nerve regeneration near the injury site and related to the damage of the myelin [27]. And CMAP amplitude represents the number of nerve fibers that respond to the stimulus and are able to deliver impulses to the recorded muscle [37]. Thus, SFI and electrophysiological examinations of injured nerve regeneration in model group remain decreased comparing to the normal side. However, the values of wet muscle weight, wet weight ratio and the cross-section area, except the diameter of muscle fiber, in model group were significantly greater than those values in control group. The difference among muscular parameters might be caused by the influence of the orientation of sectioning angle [31]. Therefore, treatment of rats with $CoCl_2$, a hypoxia mimic, could promote the recovery of SFI, muscular reservation and nerve conduction during the nerve repair (Figs. 2-4). Although the improvements of electrophysiological and behavior parameters were insignificantly different comparing to injured nerve regeneration without the treatment of $CoCl_2$, the mass

and morphology of muscle fibers were maintained, which could provide the potential to gain better recovery in specific experimental condition. These results indicated that $CoCl_2$ may serve as an important potential tool to stimulate axon regeneration.

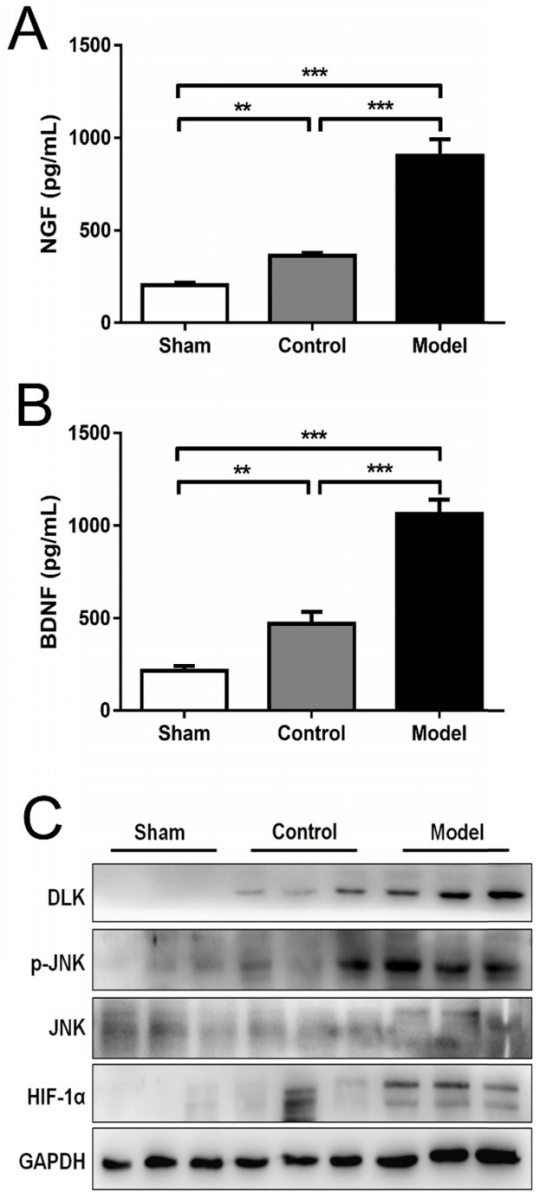

Figure 6. $CoCl_2$ significantly increased HIF-1α NGF, BDNF, DLK, JNK and p-JNK on protein level: (A-B) Qualification and comparison of protein expression of NGF and BDNF using ELISA. (C) Western blotting of nerve regeneration related proteins (HIF-1α, DLK, p-JNK and JNK) in three groups. GAPDH was used as an internal control. The data were analyzed by one-way ANOVA followed by a post-hoc method Student-Newman-Keuls (S-N-K). Graphs show indicate mean ± SD. HIF-1α: hypoxia inducible factor 1α; NGF: nerve growth factor; BDNF: brain-derived neurotrophic factor; DLK: the dual leucine zipper kinase; JNK: the c-Jun N-terminal kinase; p-JNK: phosphorylated JNK. ** $p < 0.01$. *** $p < 0.001$.

In this study, we hypothesized that $CoCl_2$, a mimic of hypoxia, may have a post-conditioning effect in nerve regeneration. The sciatic nerve injury models were established according to the method of previous study [2]. And administration of $CoCl_2$ could mimic the effect of hypoxia, which was consistent with several studies with different models [8, 40, 41]. Subsequently, it was proved that the expression of HIF-1α was significantly induced throughout the process at mRNA and protein levels. As we know, injury to the peripheral nerve axon, such as sciatic nerve, will stimulate their intrinsic growth capability [42]. It is well-known that neurotrophin and its receptor exert their significant roles in neurogenesis and neuroprotection. NGF, BDNF and GDNF are the main members that can stimulate the survival, regeneration and function of neurons [43, 44]. As previous researches reported, HIF-1α and NGF are over-expressed synergically involved in the angiogenesis [43, 45]. Nakamura et al reported that NGF-induced VEGF transcription was dependent on the increased production of HIF-1α in neuroblastoma. Lu et al found that NGF and HIF-1α were highly expressed in non-small cell lung cancer tissues as compared with para-cancerous lung tissues. In the present study, the expression of neurotrophins both on mRNA and protein level in the model group were significantly increasing compared to the control group and sham group. Here we show that HIF-1α represents an important transcriptional regulator of post-conditioning effect, with increasing levels of HIF-1α promoting the accelerated expression of neurotrophins stimulated by a prior injury. These results indicated that treatment with $CoCl_2$ may support the expression of neurotrophins during nerve regeneration *in vivo*. Future studies are needed to elucidate the relationship between neurotrophins and VEGF, as well as the effect of HIF-1α in TrkA signaling.

DLK is a component of conserved MAPK cascade that can activate the JNK families of stress MAP kinases [46]. Previous studies have indicated that the DLK promotes axonal regeneration, degeneration and neuronal cell death after nerve injury, which showed that activating the DLK pathway could be essential for axon regeneration [47-49]. In rice, DLK promotes axonal regeneration at least in part via activation of JNK and the subsequent phosphorylation [50]. Valakh et al. proved that cytoskeletal disruption activates the DLK/JNK pathway, which promotes axonal regeneration and functions as a key neuronal sensor of cytoskeletal damage [47]. The present study identified that $CoCl_2$ could significantly increase the expression of DLK, JNK and p-JNK. These results indicate that better functional recovery with treatment of $CoCl_2$ may be related to stimulate axonal skeletal repair by activation of DLK/JNK pathway.

The results of the current study need to be interpreted in light of several limitations. In this

study, considering the speed of sciatic nerve regeneration of SD rats [25, 37], we harvested the nerve and muscle tissue at 12 weeks after surgery to evaluate the functional recovery of nerve regeneration. The observations are in a specific time interval in special animal models, and therefore considering timeliness variation, topographic specificity and species differences during peripheral nerve regeneration, the results should be further confirmed in other models with further observation in long intervals. Further, owing to the differences and variations in nerve position and distribution of regeneration, although the surgery and observation was completed according to standard protocols, the result was inevitably influenced by subjective factors and system bias. Besides, whether function of reinnervated muscle after PNI can be further restored through neuronal compensation induced by HIF pathway, or whether functional recovery will decline with long-term multiple stresses, remains to be tested.

In conclusion, the results of the present study demonstrated that $CoCl_2$ enhances nerve regeneration. It was demonstrated that $CoCl_2$ induces neurotrophic factors secretion and may active HIF-1α pathway. While our results suggest that hypoxia is a viable target for the treatment of peripheral nerve transection injury.

Abbreviations

HIF-1α: Hypoxia-inducible factor-1α; $CoCl_2$: Cobalt chloride; GDNF: Glial cell line-derived neurotrophic factor; BDNF: Brain-derived neurotrophic factor; NGF: Nerve growth factor; DLK: The dual leucine zipper kinase; JNK: The c-Jun N-terminal kinase; p-JNK: Phosphorylated c-Jun N-terminal kinase; PNI: Peripheral nerve injury; RAGs: Regeneration-associated genes; SNT: Sciatic nerve transection injury; SFI: Sciatic functional index; H&E: Hematoxylin and eosin; NCV: Nerve conduction velocity; RT-qPCR: Reverse transcription-quantitative polymerase chain reaction; ELISA: Enzyme-linked immunosorbent assay; PL: Print length; TS: Toe spread; IT: Intermediary toe spread; One-way ANOVA: One-way analysis of variance.

Acknowledgments

This study was supported by Beijing Natural Science Foundation (Grant No. 7164263) and Beijing Outstanding Talents Training Project (2015000020124G116).

Author contributions statement

S.A. conceived the experiment, S.A., M.Z. and Z.L. conducted the experiment, M.F., G.C, S.L. and L.L analyzed the results. All authors reviewed the manuscript.

Competing Interests

The authors have declared that no competing interest exists.

References

1. Zhang Y, Zhan Y, Han N, Kou Y, Yin X, Zhang P. Analysis of temporal expression profiles after sciatic nerve injury by bioinformatic method. Sci Rep. 2017; 7: 9818.
2. An S, Zhang P, Peng J, Deng L, Wang Z, Wang Z, et al. Motor function recovery during peripheral nerve multiple regeneration. J Tissue Eng Regen Med. 2015; 9: 415-23.
3. Bradke F, Fawcett JW, Spira ME. Assembly of a new growth cone after axotomy: the precursor to axon regeneration. Nat Rev Neurosci. 2012; 13: 183-93.
4. Blackmore MG. Molecular control of axon growth: insights from comparative gene profiling and high-throughput screening. Int Rev Neurobiol. 2012; 105: 39-70.
5. Fagoe ND, van Heest J, Verhaagen J. Spinal cord injury and the neuron-intrinsic regeneration-associated gene program. Neuromolecular Med. 2014; 16: 799-813.
6. Moore DL, Goldberg JL. Multiple transcription factor families regulate axon growth and regeneration. Dev Neurobiol. 2011; 71: 1186-211.
7. Michaelevski I, Segal-Ruder Y, Rozenbaum M, Medzihradszky KF, Shalem O, Coppola G, et al. Signaling to transcription networks in the neuronal retrograde injury response. Sci Signal. 2010; 3: ra53.
8. Huang J, Liu L, Feng M, An S, Zhou M, Li Z, et al. Effect of CoCl(2) on fracture repair in a rat model of bone fracture. Mol Med Rep. 2015; 12: 5951-6.
9. Semenza GL. Oxygen sensing, homeostasis, and disease. N Engl J Med. 2011; 365: 537-47.
10. Semenza GL, Wang GL. A nuclear factor induced by hypoxia via de novo protein synthesis binds to the human erythropoietin gene enhancer at a site required for transcriptional activation. Mol Cell Biol. 1992; 12: 5447-54.
11. Cho Y, Shin JE, Ewan EE, Oh YM, Pita-Thomas W, Cavalli V. Activating Injury-Responsive Genes with Hypoxia Enhances Axon Regeneration through Neuronal HIF-1alpha. Neuron. 2015; 88: 720-34.
12. Lim TK, Shi XQ, Johnson JM, Rone MB, Antel JP, David S, et al. Peripheral nerve injury induces persistent vascular dysfunction and endoneurial hypoxia, contributing to the genesis of neuropathic pain. J Neurosci. 2015; 35: 3346-59.
13. Chavez JC, Almhanna K, Berti-Mattera LN. Transient expression of hypoxia-inducible factor-1 alpha and target genes in peripheral nerves from diabetic rats. Neurosci Lett. 2005; 374: 179-82.
14. Fukushima S, Endo M, Matsumoto Y, Fukushi JI, Matsunobu T, Kawaguchi KI, et al. Hypoxia-inducible factor 1 alpha is a poor prognostic factor and potential therapeutic target in malignant peripheral nerve sheath tumor. PLoS One. 2017; 12: e0178064.
15. Ho VT, Bunn HF. Effects of transition metals on the expression of the erythropoietin gene: further evidence that the oxygen sensor is a heme protein. Biochem Biophys Res Commun. 1996; 223: 175-80.
16. Nunes SC, Lopes-Coelho F, Gouveia-Fernandes S, Ramos C, Pereira SA, Serpa J. Cysteine boosters the evolutionary adaptation to CoCl2 mimicked hypoxia conditions, favouring carboplatin resistance in ovarian cancer. BMC Evol Biol. 2018; 18: 97.
17. Epstein AC, Gleadle JM, McNeill LA, Hewitson KS, O'Rourke J, Mole DR, et al. C. elegans EGL-9 and mammalian homologs define a family of dioxygenases that regulate HIF by prolyl hydroxylation. Cell. 2001; 107: 43-54.
18. Al Okail MS. Cobalt chloride, a chemical inducer of hypoxia-inducible factor-1α in U251 human glioblastoma cell line. Journal of Saudi Chemical Society. 2010; 14: 197-201.
19. Wu D, Yotnda P. Induction and testing of hypoxia in cell culture. J Vis Exp. 2011; 54: 2899.
20. Chavez JC, LaManna JC. Activation of hypoxia-inducible factor-1 in the rat cerebral cortex after transient global ischemia: potential role of insulin-like growth factor-1. J Neurosci. 2002; 22: 8922-31.
21. Dai ZJ, Gao J, Ma XB, Yan K, Liu XX, Kang HF, et al. Up-regulation of hypoxia inducible factor-1alpha by cobalt chloride correlates with proliferation and apoptosis in PC-2 cells. Journal of experimental & clinical cancer research : CR. 2012; 31: 28.
22. Ghaly A, Kok R. The effect of sodium sulfite and cobalt chloride on the oxygen transfer coefficient. Applied biochemistry and biotechnology. 1988; 19: 259-70.
23. Yuan Y, Hilliard G, Ferguson T, Millhorn DE. Cobalt inhibits the interaction between hypoxia-inducible factor-alpha and von Hippel-Lindau protein by direct binding to hypoxia-inducible factor-alpha. J Biol Chem. 2003; 278: 15911-6.
24. Shrivastava K, Bansal A, Singh B, Sairam M, Ilavazhagan G. Sub-chronic oral toxicity study in Sprague-Dawley rats with hypoxia mimetic cobalt chloride

towards the development of promising neutraceutical for oxygen deprivation. Exp Toxicol Pathol. 2010; 62: 489-96.
25. Brushart TM, Hoffman PN, Royall RM, Murinson BB, Witzel C, Gordon T. Electrical stimulation promotes motoneuron regeneration without increasing its speed or conditioning the neuron. Journal of Neuroscience. 2002; 22: 6631-8.
26. Wang Z, Zhang P, Kou Y, Yin X, Han N, Jiang B. Hedysari extract improves regeneration after peripheral nerve injury by enhancing the amplification effect. PLoS One. 2013; 8: e67921.
27. Matsuoka H, Ebina K, Tanaka H, Hirao M, Iwahashi T, Noguchi T, et al. Administration of Oxygen Ultra-Fine Bubbles Improves Nerve Dysfunction in a Rat Sciatic Nerve Crush Injury Model. Int J Mol Sci. 2018; 19, 1395.
28. Bhatt JM. The Epidemiology of Neuromuscular Diseases. Neurol Clin. 2016; 34: 999-1021.
29. Farahpour MR, Ghayour SJ. Effect of in situ delivery of acetyl-L-carnitine on peripheral nerve regeneration and functional recovery in transected sciatic nerve in rat. Int J Surg. 2014; 12: 1409-15.
30. Zhang C, Rong W, Zhang GH, Wang AH, Wu CZ, Huo XL. Early electrical field stimulation prevents the loss of spinal cord anterior horn motoneurons and muscle atrophy following spinal cord injury. Neural Regen Res. 2018; 13: 869-76.
31. Briguet A, Courdier-Fruh I, Foster M, Meier T, Magyar JP. Histological parameters for the quantitative assessment of muscular dystrophy in the mdx-mouse. Neuromuscul Disord. 2004; 14: 675-82.
32. Carroll VA, Ashcroft M. Role of hypoxia-inducible factor (HIF)-1alpha versus HIF-2alpha in the regulation of HIF target genes in response to hypoxia, insulin-like growth factor-I, or loss of von Hippel-Lindau function: implications for targeting the HIF pathway. Cancer Res. 2006; 66: 6264-70.
33. Huggett J, Dheda K, Bustin S, Zumla A. Real-time RT-PCR normalisation; strategies and considerations. Genes and immunity. 2005; 6: 279-84.
34. Mahar M, Cavalli V. Intrinsic mechanisms of neuronal axon regeneration. Nat Rev Neurosci. 2018; 19: 323-37.
35. Teoh JS, Wong MY, Vijayaraghavan T, Neumann B. Bridging the gap: axonal fusion drives rapid functional recovery of the nervous system. Neural Regen Res. 2018; 13: 591-4.
36. Murillo B, Sousa MM. Neuronal intrinsic regenerative capacity: The impact of microtubule organization and axonal transport. Dev Neurobiol. 2018; [Epub ahead of print].
37. Mekaj AY, Morina AA, Bytyqi CI, Mekaj YH, Duci SB. Application of topical pharmacological agents at the site of peripheral nerve injury and methods used for evaluating the success of the regenerative process. J Orthop Surg Res. 2014; 9: 94.
38. Alam T, Maruyama H, Li C, Pastuhov SI, Nix P, Bastiani M, et al. Axotomy-induced HIF-serotonin signalling axis promotes axon regeneration in C. elegans. Nat Commun. 2016; 7: 10388.
39. Semenza GL. Hypoxia-inducible factors in physiology and medicine. Cell. 2012; 148: 399-408.
40. Piret JP, Lecocq C, Toffoli S, Ninane N, Raes M, Michiels C. Hypoxia and CoCl2 protect HepG2 cells against serum deprivation- and t-BHP-induced apoptosis: a possible anti-apoptotic role for HIF-1. Exp Cell Res. 2004; 295: 340-9.
41. Zhou M, Lu S, Lu G, Huang J, Liu L, An S, et al. Effects of remote ischemic postconditioning on fracture healing in rats. Mol Med Rep. 2017; 15: 3186-92.
42. Neumann S, Woolf CJ. Regeneration of dorsal column fibers into and beyond the lesion site following adult spinal cord injury. Neuron. 1999; 23: 83-91.
43. Lu QL, Liu J, Zhu XL, Xu WJ. Expression of nerve growth factor and hypoxia inducible factor-1alpha and its correlation with angiogenesis in non-small cell lung cancer. Journal of Huazhong University of Science and Technology Medical sciences. 2014; 34: 359-62.
44. He Z, Jin Y. Intrinsic Control of Axon Regeneration. Neuron. 2016; 90: 437-51.
45. Nakamura K, Tan F, Li Z, Thiele CJ. NGF activation of TrkA induces vascular endothelial growth factor expression via induction of hypoxia-inducible factor-1alpha. Molecular and cellular neurosciences. 2011; 46: 498-506.
46. Hammarlund M, Nix P, Hauth L, Jorgensen EM, Bastiani M. Axon regeneration requires a conserved MAP kinase pathway. Science. 2009; 323: 802-6.
47. Valakh V, Frey E, Babetto E, Walker LJ, DiAntonio A. Cytoskeletal disruption activates the DLK/JNK pathway, which promotes axonal regeneration and mimics a preconditioning injury. Neurobiol Dis. 2015; 77: 13-25.
48. Lu Y, Belin S, He Z. Signaling regulations of neuronal regenerative ability. Curr Opin Neurobiol. 2014; 27: 135-42.
49. Yan D, Wu Z, Chisholm AD, Jin Y. The DLK-1 kinase promotes mRNA stability and local translation in C. elegans synapses and axon regeneration. Cell. 2009; 138: 1005-18.
50. Watkins TA, Wang B, Huntwork-Rodriguez S, Yang J, Jiang Z, Eastham-Anderson J, et al. DLK initiates a transcriptional program that couples apoptotic and regenerative responses to axonal injury. Proceedings of the National Academy of Sciences. 2013; 110: 4039-44.